Development of Fragility Curves for Pile foundation in Liquefied ground using Nonlinear 3D Finite Element Analysis

Partha Bhowmik[1] and Rajib Saha[2]

[1] Department of Civil Engineering, National Institute of Technology Agartala, Tripura 799046
[2] Department of Civil Engineering, National Institute of Technology Agartala, Tripura 799046

Abstract. Assessment of vulnerability of pile foundation in liquefied ground is a pertinent issue among engineering community since many failures of pile foundation were experienced in last decades due to liquefaction phenomenon. Present study is a humble attempt in this direction by estimating vulnerability of pile foundation in liquefied ground. Fragility analysis is performed to estimate vulnerability and fragility curves are accordingly developed considering different limit state criteria. Nonlinear dynamic analysis of three dimensional (3D) FEM based model of soil-pile foundation-structure system is performed using OpenseesPL software. Uncertainty modelling of ground motion is performed in a simplified manner by generating spectrum consistent artificial motions. Monte Carlo Simulation (MCS) technique is used for probabilistic analysis. Finally, the outcome of this study will help to revamp the present design guidelines of pile foundation.

1 Introduction

Failure of pile foundation was evidenced during several past earthquakes which drawn global attention to the earthquake geotechnical engineers. Failure of pile was primarily observed in soft clay or loose liquefiable deposits. Many case studies on bridge failures were reported in liquefied soil due to pile failure. Maymand (1998) presented several case study failures of pile foundation supported structures during past earthquake events. Different hypothesis about failure mechanism of pile foundation during seismic event were emerged. Bhattacharya *et al*. 2008 presented bending-buckling theory to define failure mechanism of pile. The case study of Showa bridge failure during 1964 Niigata earthquake was presented in this study. Further, another recent study by the same group (Bhattacharya *et al*. 2014) has concluded that bending-buckling theory sole cannot explain the failure mechanism of pile of Showa Bridge and suggested resonating response of the whole structure would be governing factor to expedite bending-bucking interaction, which lead to failure of the pile before commencement of lateral spreading event. On the other hand, many researchers claimed that bridge failure has occurred only due to significant bending moment developed at pile head due to lateral spreading caused during liquefaction occurrence (Hamada *et al*. 1992, Kramer *et al*. 1996, Bhattacharya *et al*. 2003, Tokimatsu *et al*.

2005. In addition, failure of bridge structures supported by pile foundation is not only limited to liquefaction but also other ground damage including landslide and excessive lateral displacement (Boulanger *et al*. 1995; Miller and Roycroft 2004; Audemard *et al*. 2005; Sonmez *et al*. 2008; Palermo *et al*. 2011; Haskell *et al*. 2013). Furthermore, the differential settlement occurred to the engineering structure supported on pile due to flow liquefaction are also observed in many earthquake events (1964 Alaska earthquake, 1990 Luzon earthquake, 1991 Costa Rica earthquake, 1976 Tangshan Earthquake, the 1994 Northridge Earthquake, 1995 Kobe Earthquake). From this above point of view, it has been realized that vulnerability assessment of pile foundation, mainly in liquefiable deposit is indispensable. It is also observed that seismic vulnerability of structure is represented by constructing fragility curves. Zentner *et al.* 2016 discussed different methods for developing fragility curves and described their advantages and disadvantages and out of those multiple strips analysis (MSA) is most reliable method for uncertainty analysis. Input motion characteristics have significant effect on vulnerability curves (Kwon *et al*. 2005 , Zhang *et al.* 2008).

In this context, present study is an effort to assess the vulnerability of pile foundation embedded in liquefaction susceptible layer by performing probabilistic nonlinear dynamic analysis of a 3D finite element based model of soil-pile foundation-structure system. Nonlinear 3D FEM analysis is performed in OPENSeesPL (*V 2.7.2*, 2018).The case study of Showa bridge pile foundation is used in present analysis. Fragility analysis is performed by incorporating variability of ground motions having peak ground acceleration (PGA) within a range of 0.005g to 1.1g Fragility curves are generated based on the 'failure' and 'success' information gathered from comparisons using multiple strip analysis in which maximum likelihood method helps for best fitting of fragility curves. Vulnerability of pile foundation is presented as cumulative density function (CDF) of probability of failure (POF) with respect to both collapse and serviceability limit state criteria. Furthermore, POF with respect to ductility demand of pile also reported herein. Monte Carlo Simulation (MCS) is used to calculate POF. Keeping view on the failure mechanism of pile foundation, both inertial and kinematic interaction under seismic loading are considered during the analysis for assessing vulnerability of pile foundation attributing different failure mechanisms. Hence, the outcome of present study will help to provide significant design inputs for design of pile foundation in liquefiable soil.

2 Modeling of Soil Pile System

2.1 Pile modeling

The case study of Showa bridge in Japan which damaged during 1964 Niigata earthquake is considered in present study. Details of Showa bridge is available elsewhere (Bhattacharya *et al*. 2014). The 25 m long pile passes through a four-phase system of air, water, liquefied soil, and non-liquefied soil surrounding it.The first 10 m soil is medium to coarse sand (N 10) and second 6 m is dense sand (N 30). 3D finite element model of soil-pile system is modelled in OpenseesPL (*V*.2.7.2, 2018) as shown in Figure 1. 1×3 pile group is modelled instead of actual 1×9 group due to

limitation of nodes in education version of OpenseesPL (*V*.2.7.2, 2018). However, all other parameters related to geometric and material properties of pile are kept same as per Bhattacharya *et al*. (2014). Total dead and live load acting on pile head is calculated as 800 kN for each pile. Accordingly, axial load is calculated for 1×3 pile group which is further used in analysis. Table 1 presents the detailed parameters of pile and soil.

Table 1. Properties of pile used in this study

Pile Parameters	Values
Pile Diameter (m)	0.353
Pile Length (m)	25
Young's Modulus (GPa)	210
Section Modulus (m^3)	0.0015
Flexural strength of pile (MPa)	490
Ultimate moment capacity of pile (kN-m)	1286
Plastic Moment capacity of pile (kN-m)	2415
Flexural Rigidity (kN-m2)	160061.92
Shear Rigidity (kN)	9063516
Torsional Rigidity (kN-m2)	1133228
Axial Rigidity (kN)	23562000
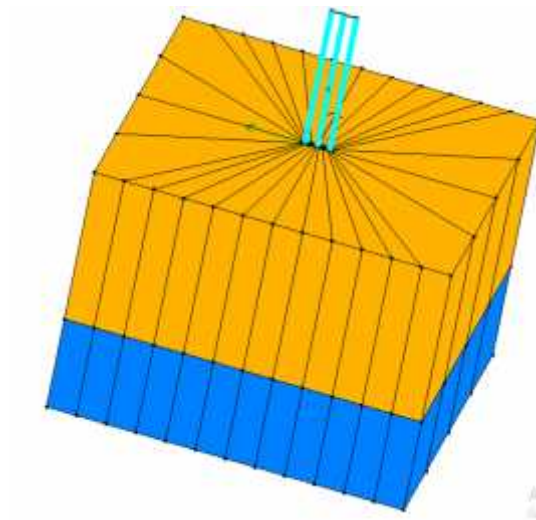
Fig. 1. Numerical model of soil-piled structure system modeled in OpenseesPL 2.7.2

4

The pile group system embedded in liquefaction susceptible ground is modelled with and without axial load in order to simulate inertial and kinematic interaction respectively. Figure 2 presents schematic idealization of both the interactions analysed in present study. The pile is modeled using displacement based beam column element having 3D fibre section with 8 number of splices. Nonlinear elasto-plastic material is assigned for pile element. The tip of pile is assigned with fixed boundary condition with the assumption that pile will undergo zero vertical settlement.
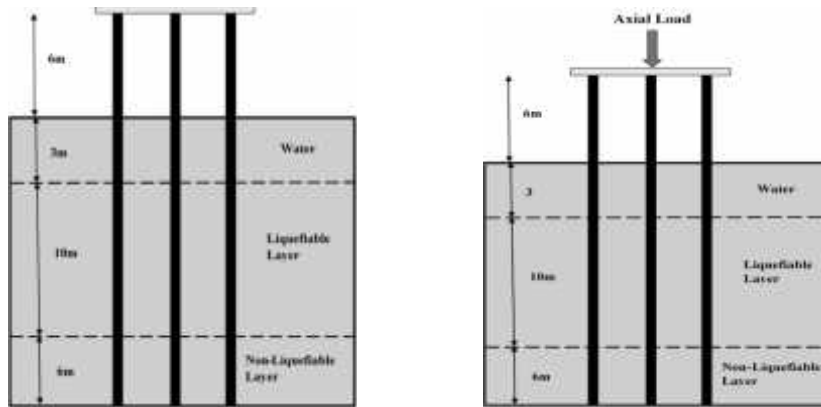
Fig. 2. Schematic idealization of model of Showa Bridge pile and soil profile (a) Without loading condition (b) With loading condition.

2.2   Soil domain modeling

The dimension of soil domain is considered as 20 m long, 11 m wide and 10 m thick. In finite element modelling of foundation soil is modeled using *Pressure Depend Multi Yield* material. Soil domain is discretized by 3D 8 nodded brick element having 3 DOF at each node. The consistency of soil is medium to coarse sand up to a depth of 10m. However the consistency changes to dense condition with a depth below 10m. The properties of different soil stratum are presented in Table 2. The lateral boundary is considered as periodic boundary whereas the bottom layer below pile is assumed as rigid. Damping ratio of 5% of critical damping is applied for pile-soil system irrespective of mode of vibration. The 3D brick element representing soil mass are connected to 1D pile element by rigid links through zero length element and equal translation constraint (i.e., *equalDOF* option in OpenSeesPL).

**Table 2**. Properties of soil used in this study

Soil Parameters	Liquefiable Layer (10m)	Non-Liquefiable layer (6m)
N value	<10	>30
Saturated mass density (Mg/m3)	1.7	2.1
Shear Modulus (kPa)	55000	130000
Relative Density	40%	>75%
Friction Angle	29°	40°

3   Uncertainty modeling of Ground Motion

Present study models uncertainty of ground motion using a simplified technique suggested by Haldar (2009) who mentioned the variability associated with elastic response spectrum ordinates can be divided into three main classes as seismic source and attenuation variability (σ_{SE}), variability due to local geology and site condition (σ_{GS}) and variability associated with seismic force determination (σ_{RS}). The value of σ_{SE} in this study is assumed as 0.001g. The variability due to σ_{GS} is taken as 0.004g considering category of soil as class A (IS1893 Part 1 2016). The variability due to σ_{RS} is assumed as 0.003g considering variability in modeling uncertainty. These three categories of variability are combined to determine the resultant variability (σ_R) of the response spectrum ordinate, which is further utilized to determine the variability in the ground motion. The resultant variability (σ_R) is presented as follows,

$$\sigma_R = \sqrt{\sigma_{SE}^2 + \sigma_{GS}^2 + \sigma_{RS}^2} \tag{1}$$

Present study considers Indian Standard (IS) spectra for Soft soil as mean spectra considering 5% damping and COV of 5%. Figure 3 presents randomly generated 30 realizations of response spectrum curve considering IS 1893-Part 1-2002 spectra as mean curve and following rest other assumed statistical parameters.
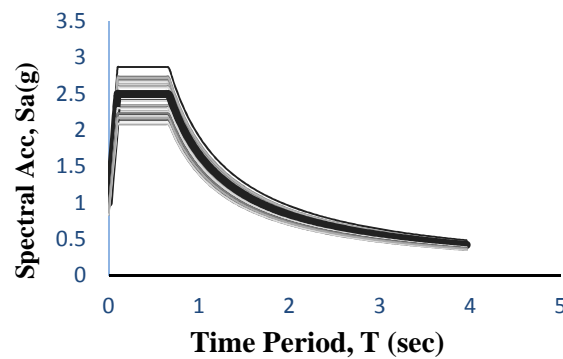
Fig. 3. Randomly generated response spectra as per IS 1893-Part 1-2016.

For each spectrum curve, a set of eight artificial motions are generated and finally a total of 240 numbers of ground motions are obtained for analysis. One randomly generated ground motion from Spectral ordinates for zero period 0.651g spectral acceleration is shown in figure 4.
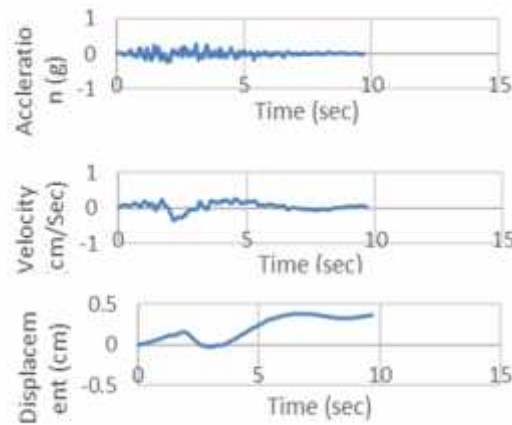
Fig. 4. Representative artificially generated synthetic ground motion

4 Method of Analysis

Nonlinear dynamic analysis is performed on 3D finite element modelling of soil-pile group system.The incremental iterative procedure proposed by *Newark's* - time stepping method with time integration parameters =6 and =0.3025 is used to integrate equation of motion. Krylov-Newton algorithm is considered to carry out the analyses for large number of DOFs. Initial tangent stiffness of the system is set for all the analysis and iterations and near about 40-50 iterations for every case are needed to achieve convergence tolerance (displacement increment) of 10^{-6}.

In this study, the numerical model is analyzed for each spectral level i.e. with eight ground motions. For each intensity level, number of failures out of eight analysis gives the probability of failure for that level. Therefore, with the increasing of intensity level the fraction causing collapse is also increasing. The fitting technique adopted is the method of maximum likelihood, noted by a number of authors (Shinozuka et al. 2000;Baker and Cornell 2005). Failure state i.e. limit state is defined as maximum lateral displacement of 30 mm for serviceability state as per Das *et al*. 2016 and ultimate moment carrying capacity shown in table 3 is considered as collapse state.

Table 3. Limit states in terms of Collapse and Serviceability

Limit states	Criteria	Values
Collapse state	Max. resisting moment M_y, kN-m	1280
Serviceable state	Max. Pile head displacement, mm	30

Calculating the number of failures at each of 30 different spectrum level helps in developing the fragility curves. Therefore, for four cases of vertical loading condition (0%, 33%, 67%, 100%) a total number of 960 analysis is carried out.

5 Results and Discussion

The accuracy and correctness of a FE model used has been validated for maximum ground displacement. In this study maximum ground displacement of 20 cm is found when the FE model is analyzed with N-S component of Niigata motion shown in figure 5. As per Bhattacharya *et al.* 2014, the maximum soil displacement at the recording site in the direction of bridge (30° North-West) is about 22cm. So this indicates a well agreement with the results obtain in the present study.
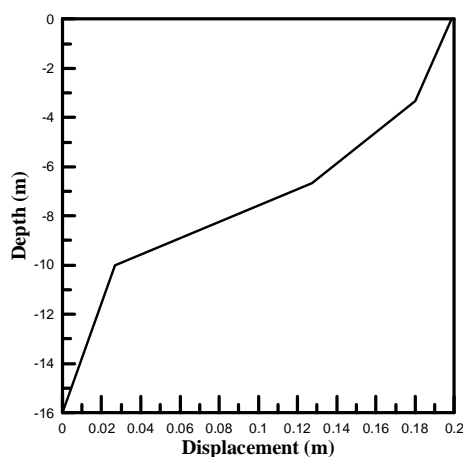

Fig. 5. maximum soil displacement profile of single pile numerical model for Niigata N-S component

In single motion analysis, fragility curves are developed for 4 cases of vertical loading conditions such as 0%, 33%, 66%, 100% (shown in figure 5 to 8 respectively) considering serviceability as well as collapse state.
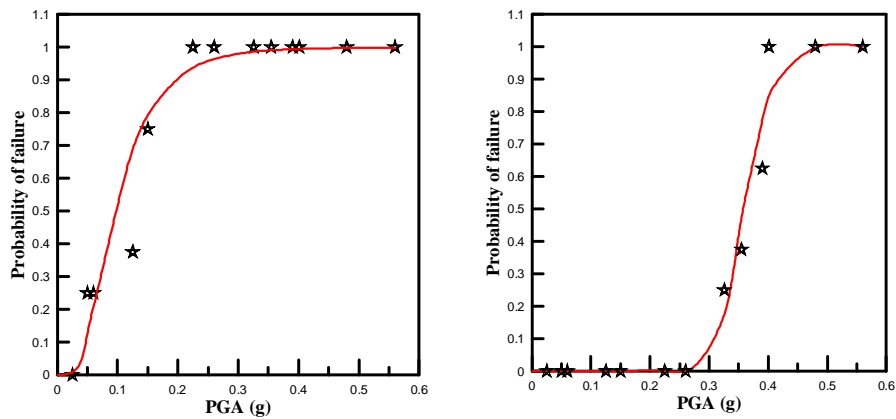
8
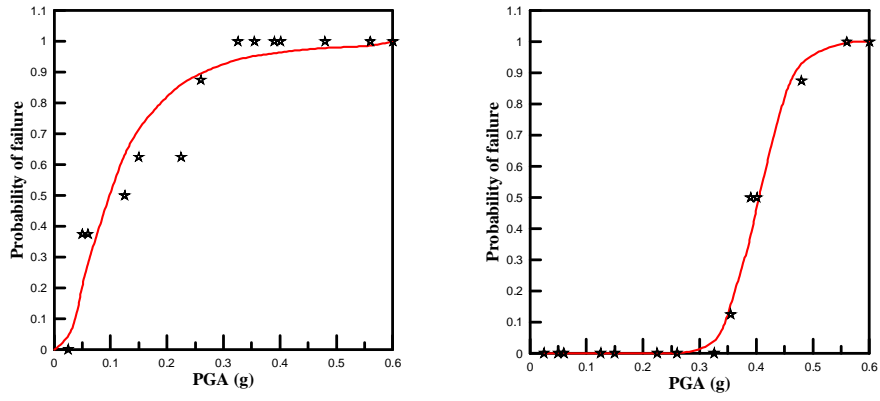
Fig. 5. Fragility curves for zero load condition (a) Serviceability State (b) Collapse State
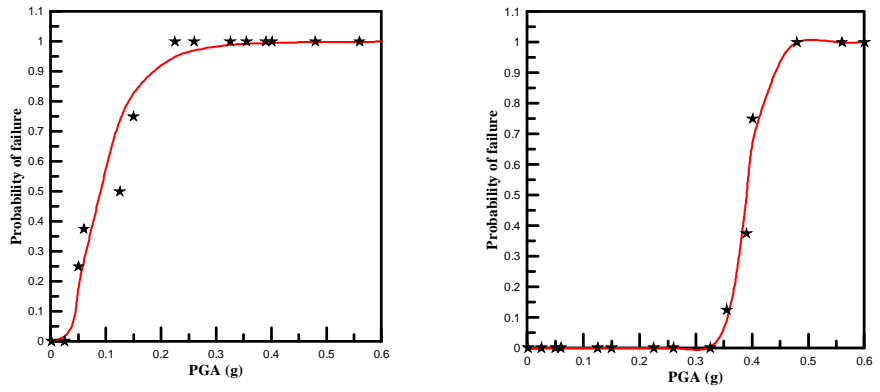
Fig. 6. Fragility curves for 800KN (33%) load condition (a) Serviceability State (b) Collapse State
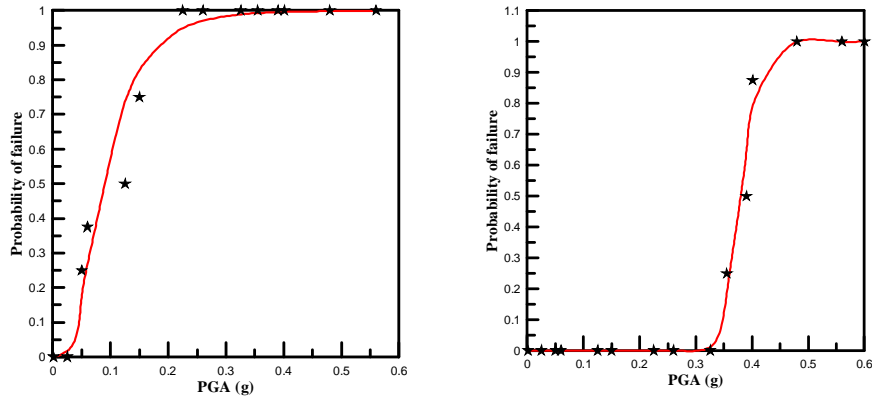
Fig. 7. Fragility curves for 1600KN load(67%) condition (a) Serviceability State (b) Collapse State

Fig. 8. Fragility curves for 2400KN (100%) load condition (a) Serviceability State (b) Collapse State.

The numerical model developed in present study using OPENSeesPL (*V*-2.7.2, 2018) is validated with physical observations of Showa bridge site after 1964 Niigata earthquake which indicates a well agreement with the results obtained from present study. Based on this validation study, the 3D soil-pile foundation system modeled in OPENSeesPL (*V*-2.7.2, 2018) is used in further analysis of present study. Fragility curves are developed for both serviceability and collapse criteria attributing 0%, 33%, 67% and 100% of axial load. Results indicate that probability of failure is higher pertaining to serviceability limit state as compared to collapse criteria. For instance, POF reaches 100% at PGA of 0.40g and 0.60g considering serviceability and collapse criteria

respectively in case of zero percentage of axial loading. Similar trend is observed irrespective of all loading cases. Further, it is observed that POF attains 100% at relatively lower PGA when axial loading increases which may be due to P-Δ effect.

References

1. Bea, R.G. 1999. "Reliability based Earthquake design guidelines for marine structures", *Journal of Waterway, Port, Coastal and Ocean Engineering*, ASCE, Vol.125 (5),219-231.
2. Bhattacharya S, Dash SR, Adhikari S. "On the mechanics of failure of pile-supported structures in liquefiable deposits during earthquakes". CurrSci 2008b;94(5):605–11.
3. BhattacharyaS, Tokimatsu K. "Collapse of Showa Bridge revisited" .Int J Geoeng Case Hist 2013;3(1):24–35.
4. Bhattacharya, S. Tokimatsu, K.Goda, K.Sarkar, R.Shadlou, M. Rouholamin, M. 2014. "Collapse of Showa Bridge during 1964 Niigata earthquake: A quantitative reappraisal on the failure mechanisms", *Soil Dynamics and Earthquake Engineering*, 65 (2014) 55–71.
5. Boulanger RW, Idriss IM, Mejia LH (1995) . "Investigation and evaluation of liquefaction related ground displacements at Moss Landing during the 1989 Loma Prieta Earthquake". Center for Geotechnical Modeling, Department of Civil & Environmental Engineering, University of California.
6. Haldar, S. Babu, G.L.S, "Probabilistic Seismic Design of Pile Foundations in Non-Liquefiable Soil byResponse Spectrum Approach", *Journal of Earthquake Engineering*, 13:737–757, 2009.
7. Hamada M, O'Rourke TD. "Case studies of liquefaction and lifeline performance during past earthquakes. Japanese case studies", Technical Report NCEER-92- 0001; 1992.
8. Haskell J, Madabhushi S, Cubrinovski M, Winkley A (2013). Lateral spreading-induced abutment rotation in the 2011 Christchurch earthquake: Observations and analysis. Geotechnique, 63(15): 1310-1327.
9. Kumar C.M.R, Narayan K.S.B, Reddy D. Venkat (2014). "Methodology for Probabilistic Seismic Risk Evaluation of Building Structure Based on Pushover Analysis." *Open Journal of Architectural Design*, 2(2):13-20.
10. Kwon, O.S. Elnashai, A. "The effect of material and ground motion uncertainty on the seismic Vulnerability curves of RC structure", Engineering Structures, 28 (2006) 289–303.
11. Meymand, P. J (1998). "Shaking table scale model tests of nonlinear soil-pile-superstructure interaction in soft clay". (Doctoral dissertation, University of California, Berkeley).
12. Miller EA, Roycroft GA (2004). "Seismic performance and deformation of levees: four caseStudies". *Journal of Geotechnical and Geoenvironmental Engineering*, 130(4): 344-354.
13. Sonmez B, Ulusay R, Sonmez H (2008). "A study on the identification of liquefaction-inducedfailures on ground surface based on the data from the 1999 Kocaeli and Chi-Chi earthquakes".Engineering Geology, 97(3): 112-125.
14. Tokimatsu K, Suzuki H, Sato M. "Effects of Inertial and kinematic interaction on seiasmic behavior of pile with embedded foundation". *Soil Dynamics and Earthquake Engineering* 2005;25(?):753–62.
15. Zhang, J. Huo, Y. Brandenberg, S.J. Kashighandi, P. 2008. "Fragility Functions of Different Bridge Types Subject to Seismic Shaking and Lateral Spreading". The 14th World Conference on Earthquake Engineering, Beijing, China.